Central European Journal of Energetic Materials
ISSN 1733-7178; e-ISSN 2353-1843
Supplementary Information (SI) for *Cent. Eur. J. Energ. Mater.* **2020**, *17*(4): 584-599

Supplementary Information is available in PDF-format at:
http://www.wydawnictwa.ipo.waw.pl/cejem/Vol-17-Number4-2020/CEJEM_01119_SI.pdf

Article is available under the Creative Commons Attribution-Noncommercial-NoDerivs 3.0 license CC BY-NC-ND 3.0.

Supplementary Information

Please note:
1) The publisher is not responsible for the content of the section Supporting Information.
2) Any queries should be directed to the corresponding Author mentioned below.

Research paper

The Shooting Tests of Target Perforating Ability, Performed on Cast Concrete Cylinders

Łukasz Habera[1], Kamil Hebda[1], Piotr Koślik[2], Tomasz Sałaciński[3]
[1] *Oil and Gas Institute – National Research Institute, 25 A Lubicz Street 6, 31-503 Cracow, Poland*
[2] *Łukasiewicz Research Network – Institute of Industrial Organic Chemistry, Branch in Krupski Młyn, 1 Zawadzkiego Street, 42-693 Krupski Młyn, Poland*
[3] *Łukasiewicz Research Network – Institute of Industrial Organic Chemistry, 6 Annopol Street, 03-236 Warsaw, Poland*
* *E-mail:* habera@inig.pl

Figure S1. Concrete cores (target models) and, at the front, core No. 8 with the shaped charge attached

(a)

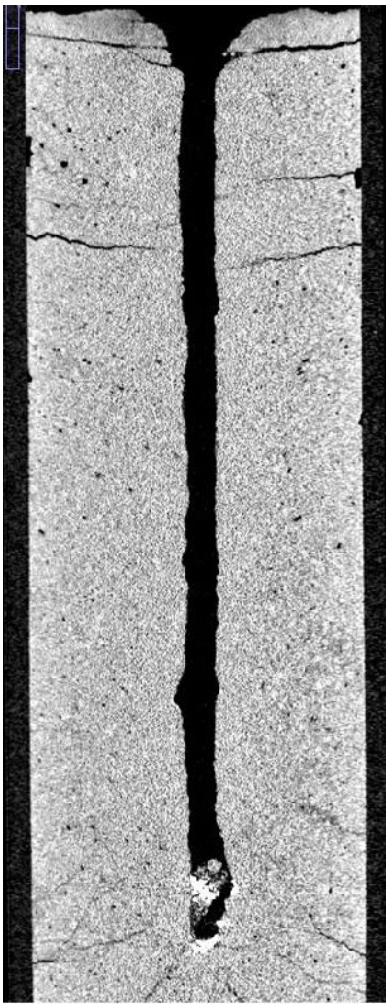

(b)

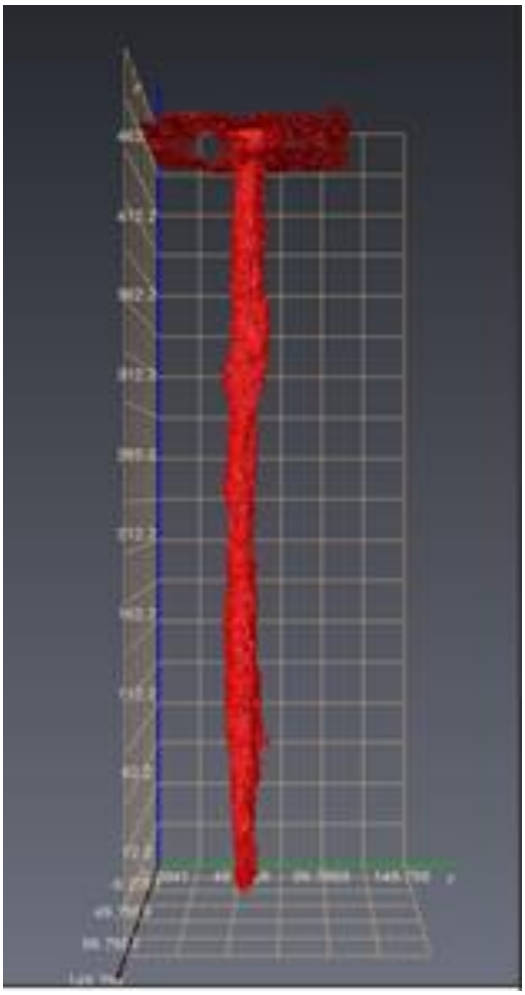

(c)

Figure S2. Test No. 2 (Series EP): view from the top (a), XCT image of the perforated concrete core (b), and 3D view of the perforation channel (c)

(a)

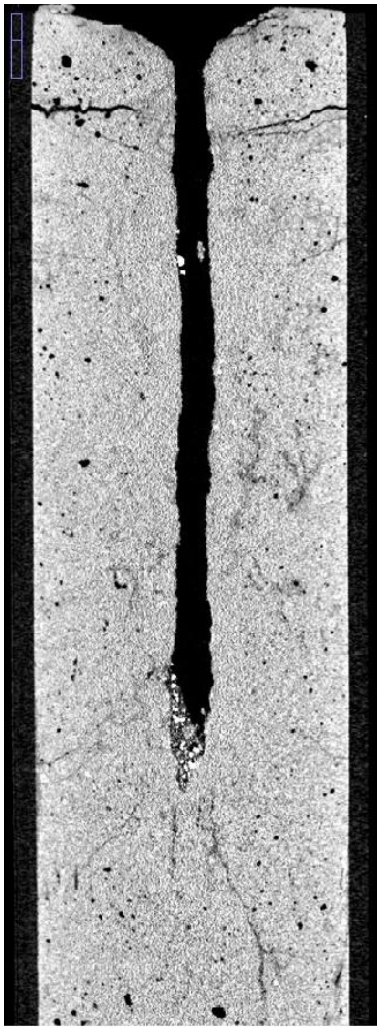

(b)

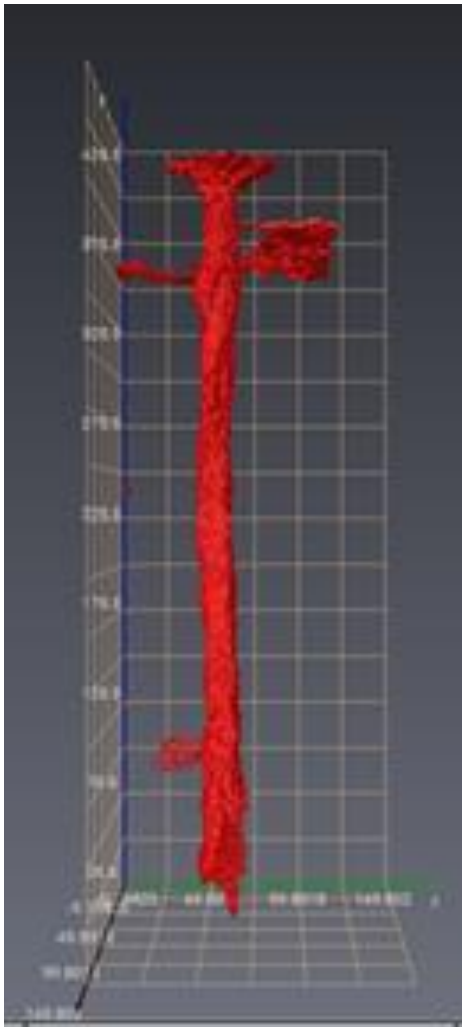

(c)

Figure S3. Test No. 3 (Series EP): view from the top (a), XCT image of the perforated concrete core (b), and 3D view of the perforation channel (c)

(a)

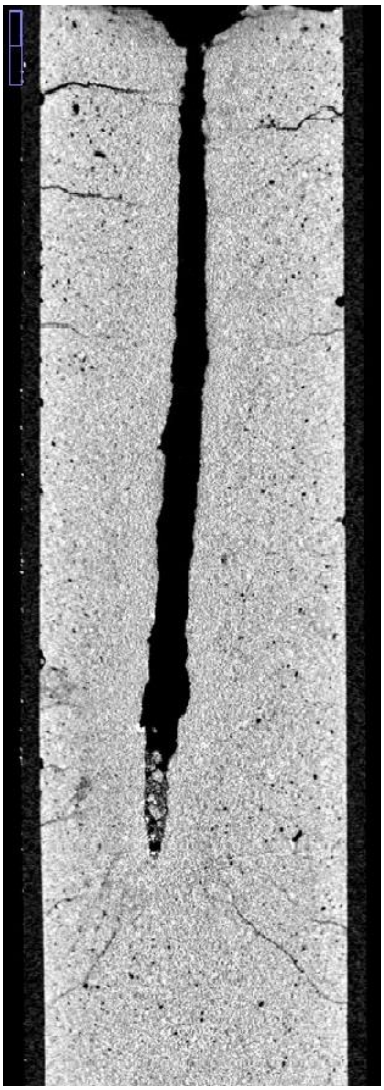

(b)

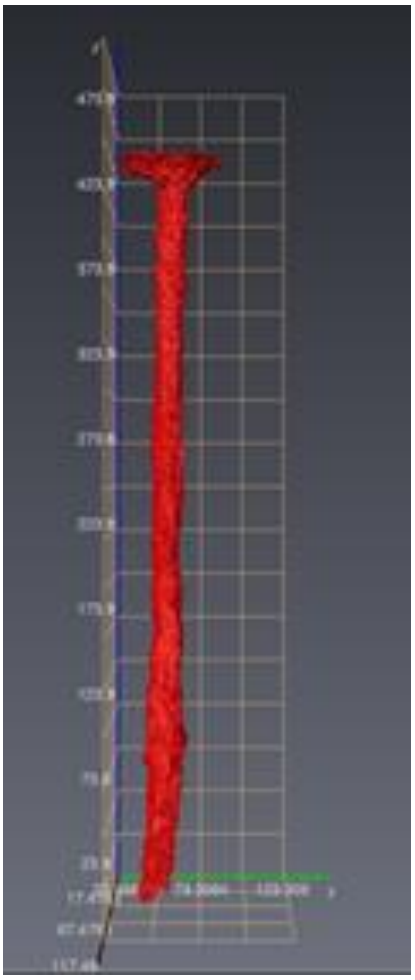

(c)

Figure S4. Test No. 4 (Series EP): view from the top (a), XCT image of the perforated concrete core (b), and 3D view of the perforation channel (c)

(a)

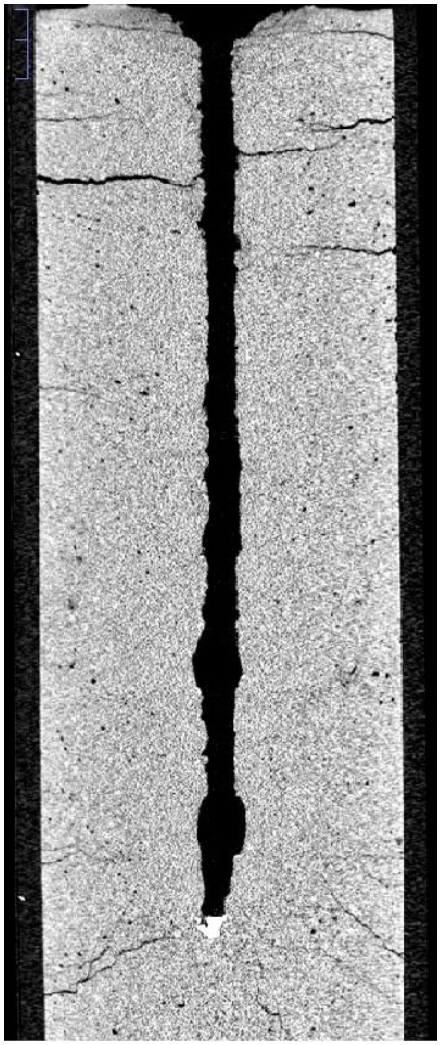

(b)

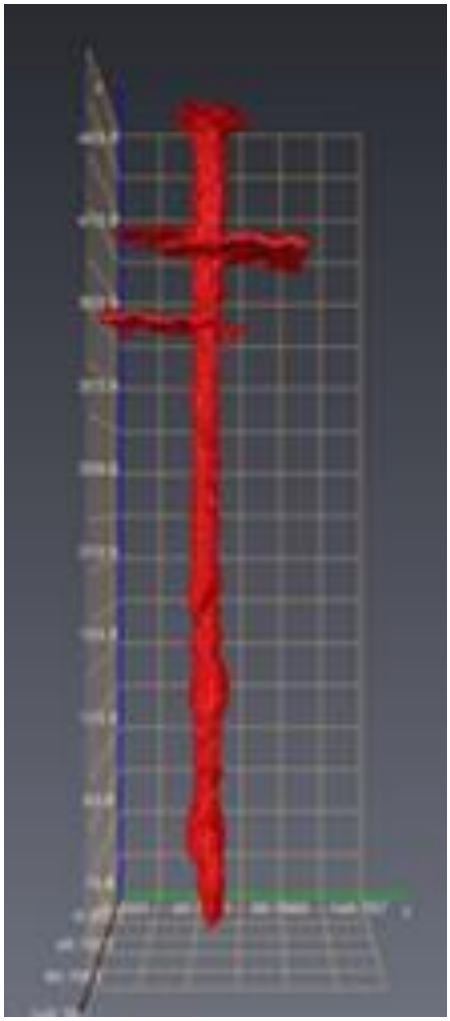

(c)

Figure S5. Test No. 5 (Series EP): view from the top (a), XCT image of the perforated concrete core (b), and 3D view of the perforation channel (c)

(a)

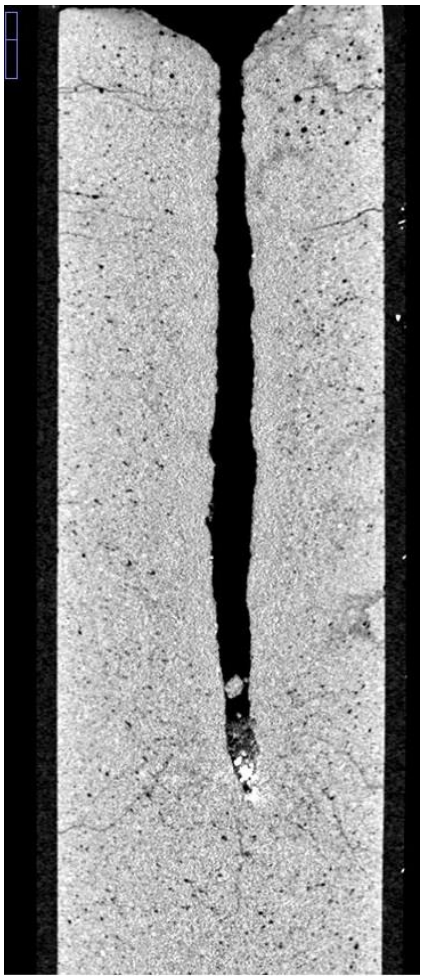

(b)

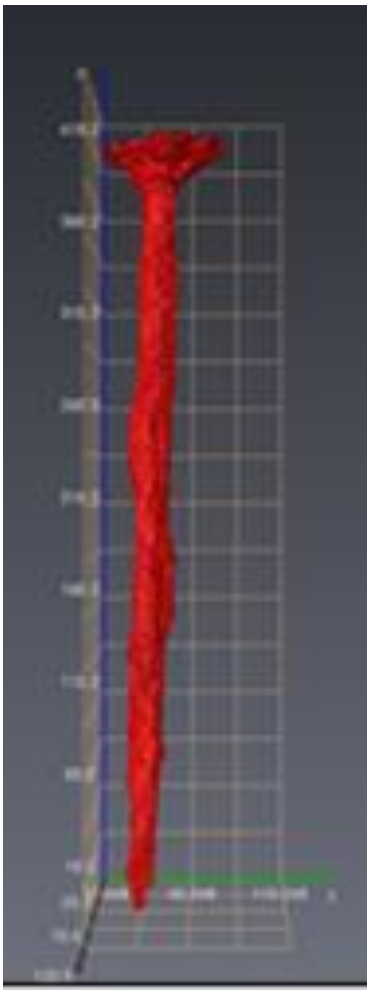

(c)

Figure S6. Test No. 6 (Series EP): view from the top (a), XCT image of the perforated concrete core (b), and 3D view of the perforation channel (c)

(a)

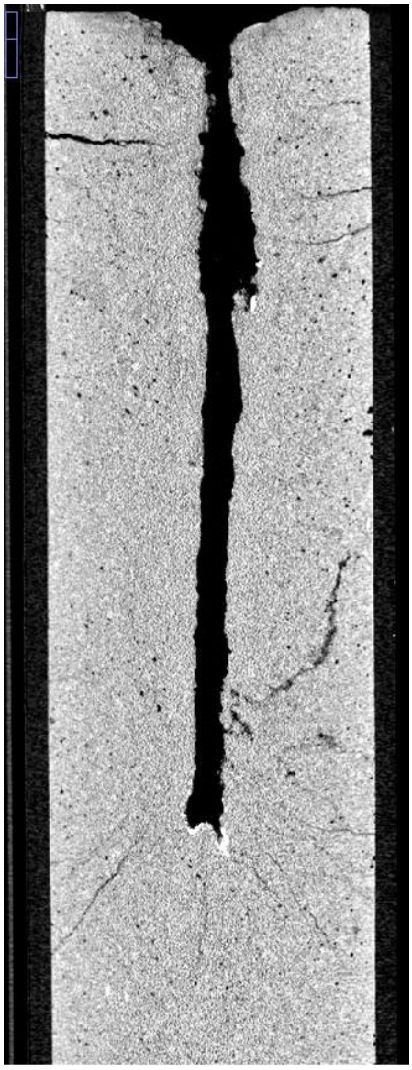

(b)

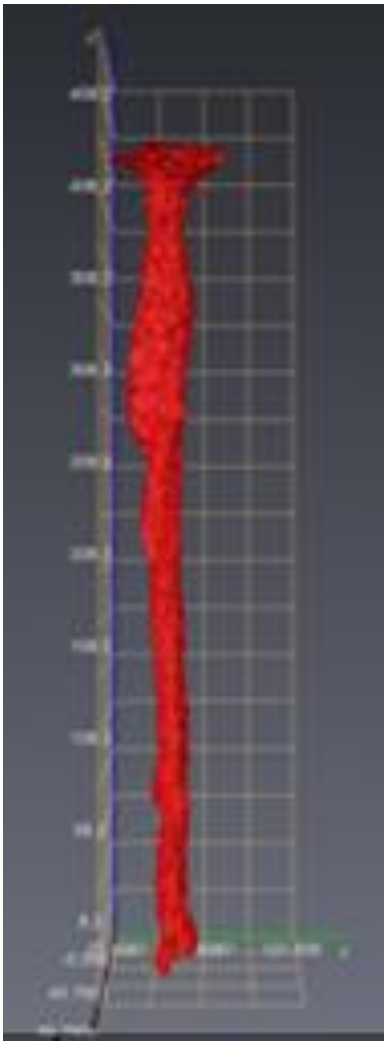

(c)

Figure S7. Test No. 7 (Series EP): view from the top (a), XCT image of the perforated concrete core (b), and 3D view of the perforation channel (c)

(a)

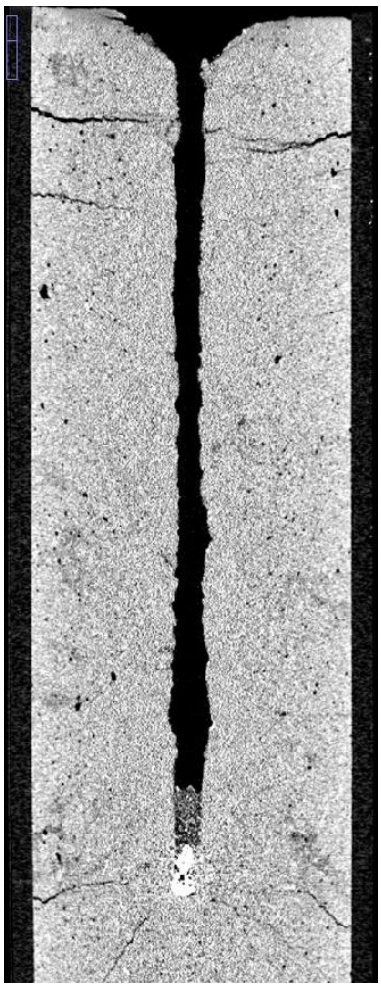

(b)

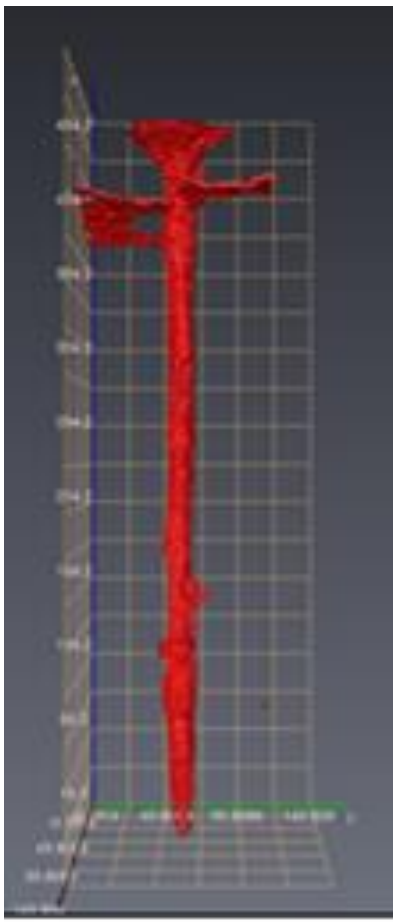

(c)

Figure S8. Test No. 8 (Series EP): view from the top (a), XCT image of the perforated concrete core (b), and 3D view of the perforation channel (c)

(a)

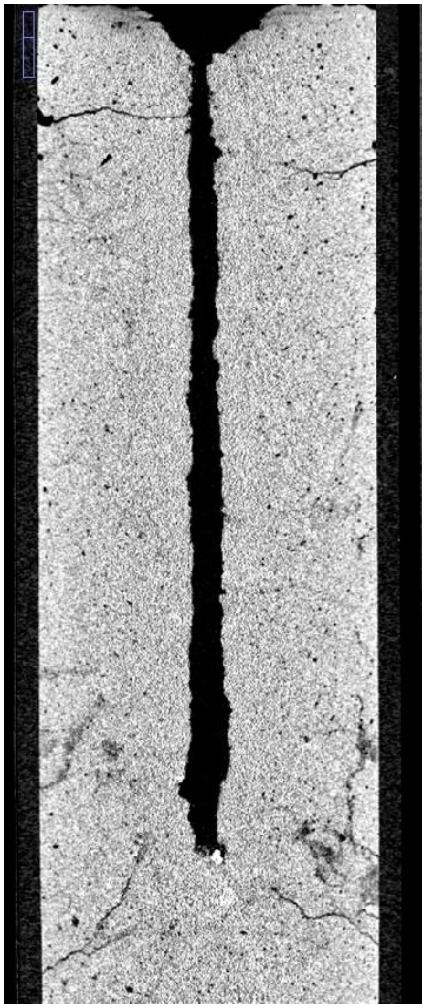

(b)

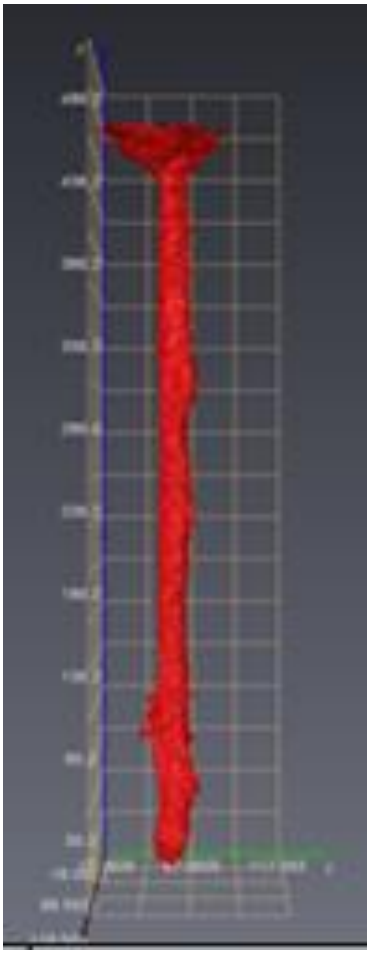

(c)

Figure S9. Test No. 9 (Series EP): view from the top (a), XCT image of the perforated concrete core (b), and 3D view of the perforation channel (c)

(a)

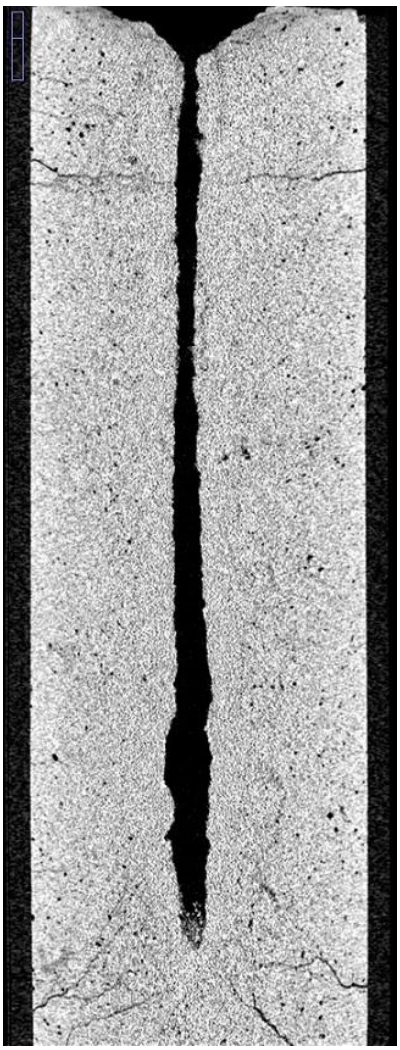

(b)

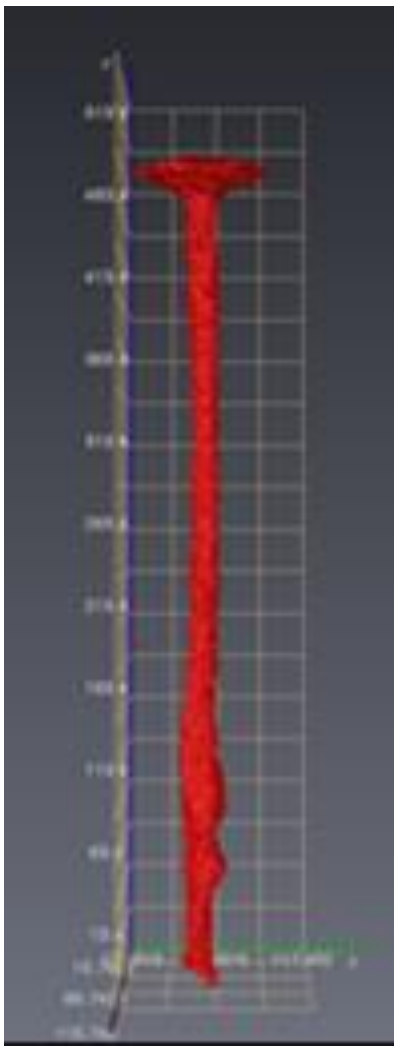

(c)

Figure S10. Test No. 10 (Series EP): view from the top (a), XCT image of the perforated concrete core (b), and 3D view of the perforation channel (c)

(a)

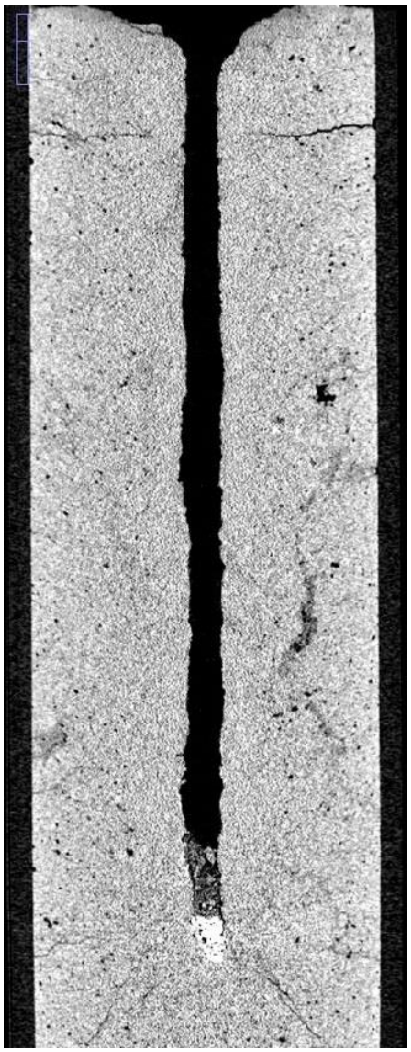

(b)

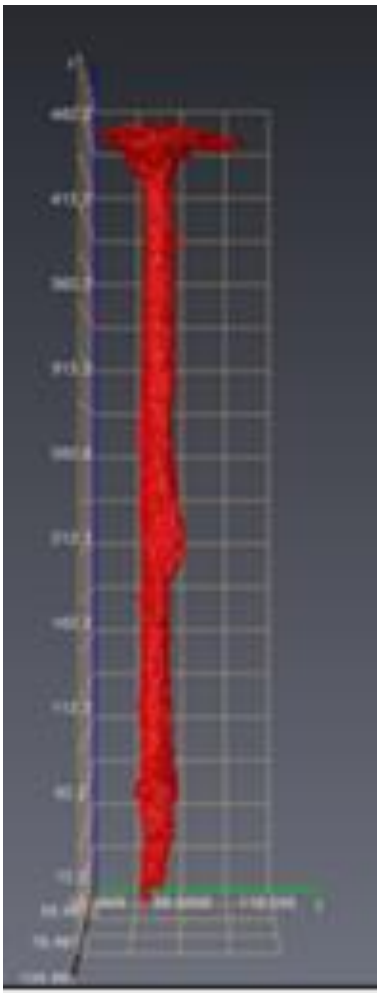

(c)

Figure S11. Test No. 11 (Series EP): view from the top (a), XCT image of the perforated concrete core (b), and 3D view of the perforation channel (c)

(a)

(b)

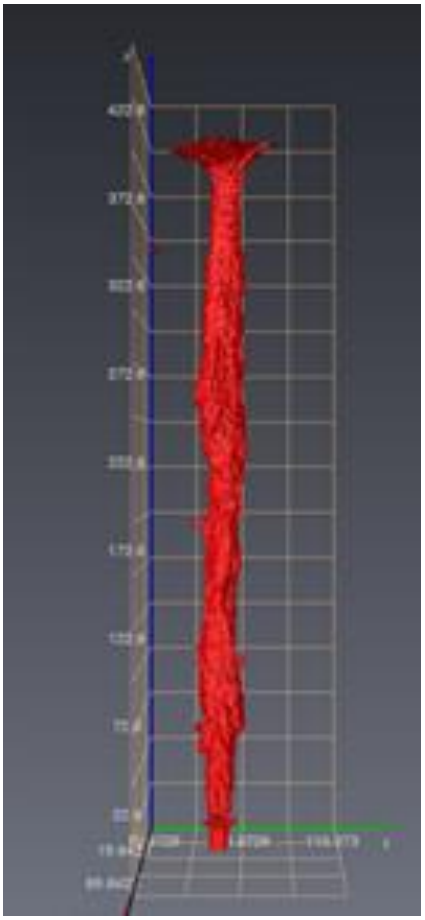

(c)

Figure S12. Test No. 13 (Series EW): view from the top (a), XCT image of the perforated concrete core (b), and 3D view of the perforation channel (c)

(a)

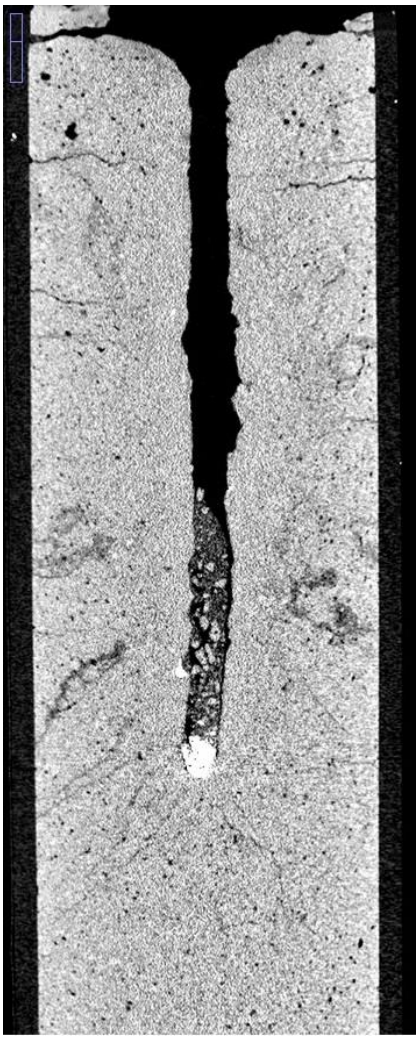

(b)

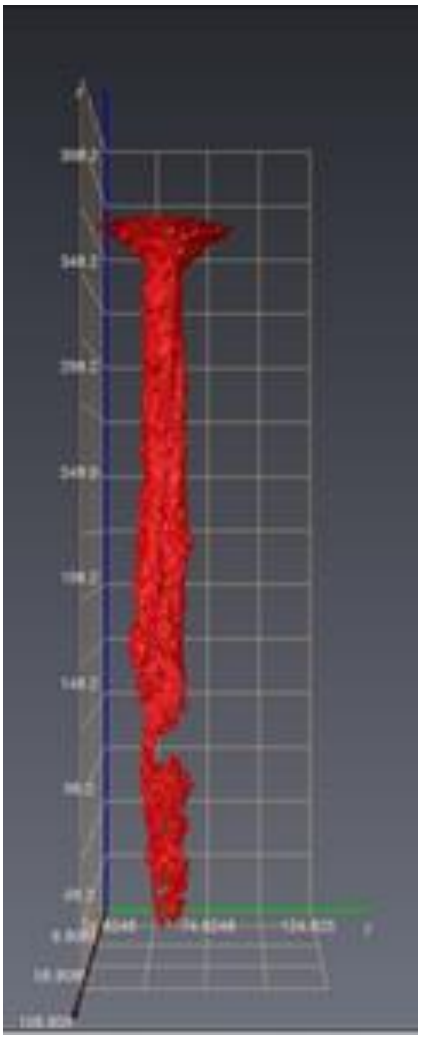

(c)

Figure S13. Test No. 14 (Series EW): view from the top (a), XCT image of the perforated concrete core (b), and 3D view of the perforation channel (c)

(a)

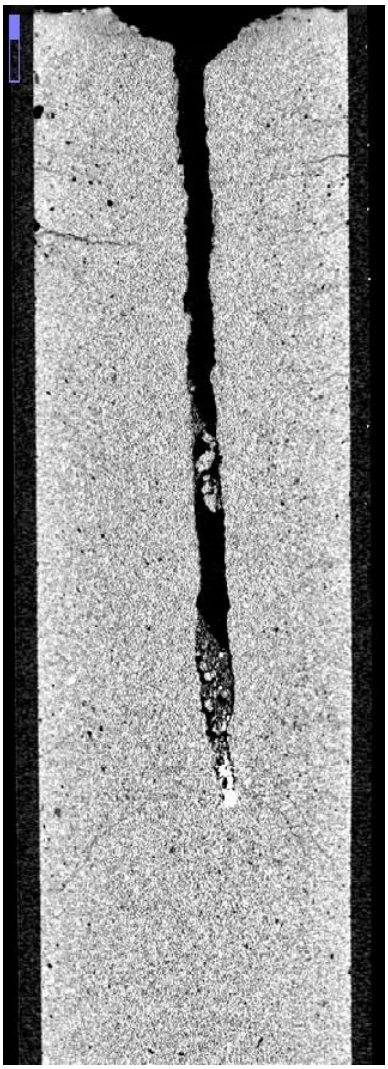

(b)

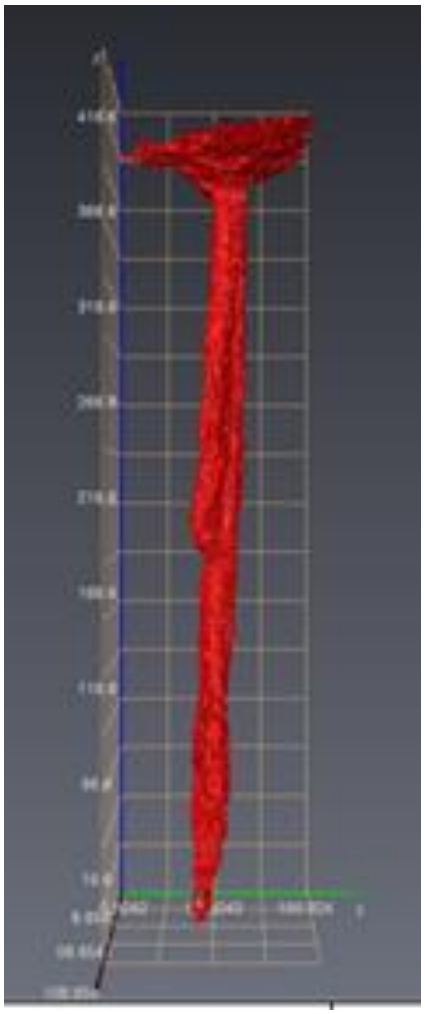

(c)

Figure S14. Test No. 15 (Series EW): view from the top (a), XCT image of the perforated concrete core (b), and 3D view of the perforation channel (c)

(a)

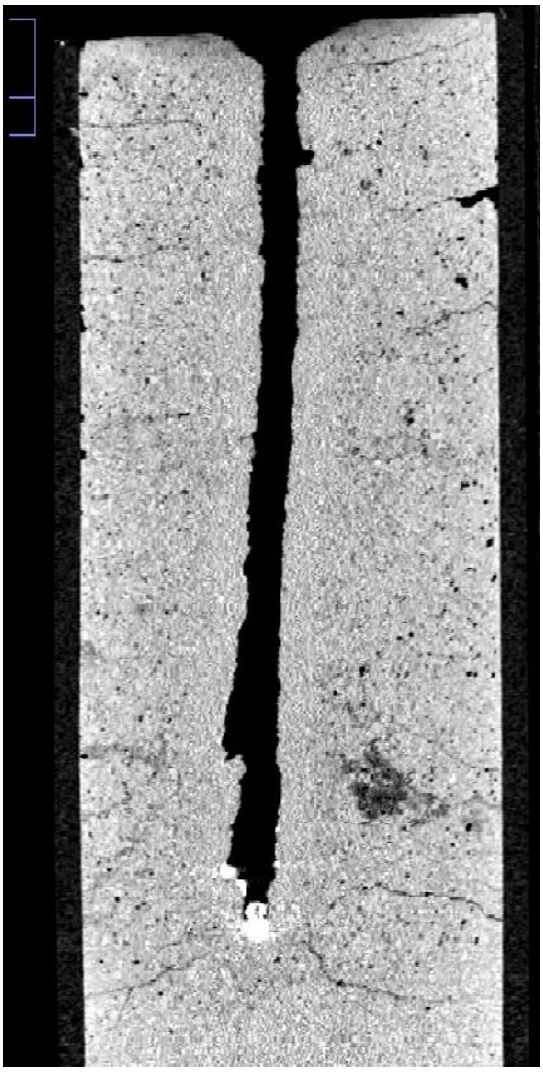

(b)

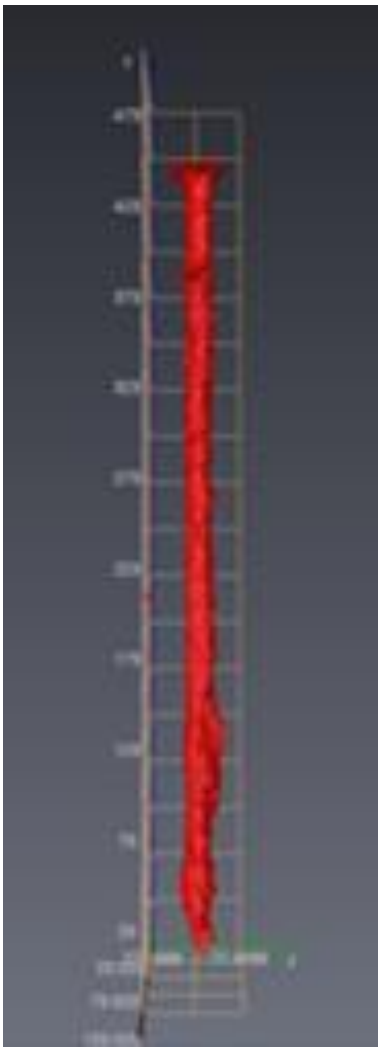

(c)

Figure S15. Test No. 16 (Series EW): view from the top (a), XCT image of the perforated concrete core (b), and 3D view of the perforation channel (c)

(a)

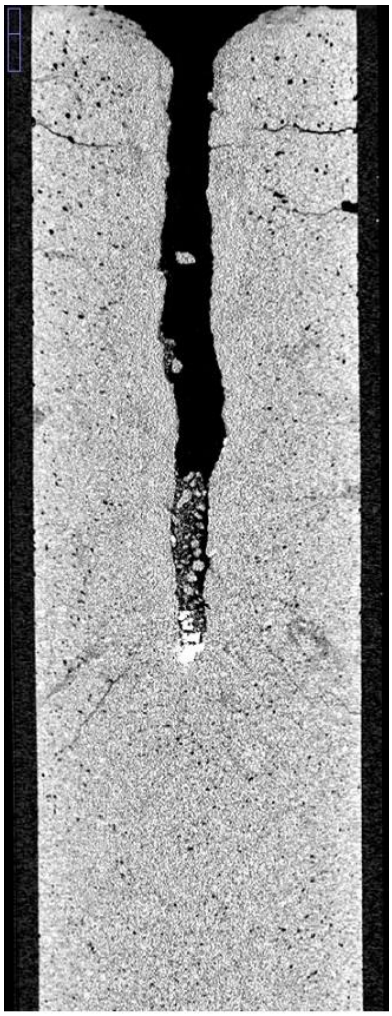

(b)

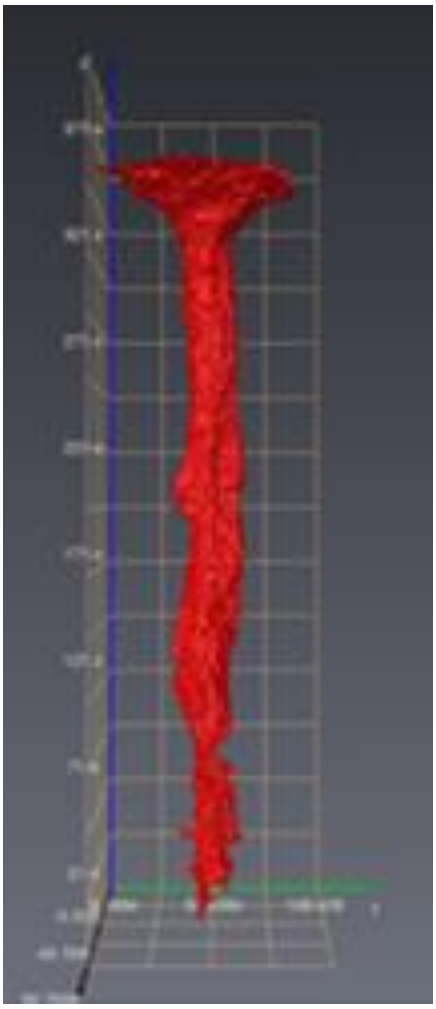

(c)

Figure S16. Test No. 17 (Series EW): view from the top (a), XCT image of the perforated concrete core (b), and 3D view of the perforation channel (c)

(a)

(b)

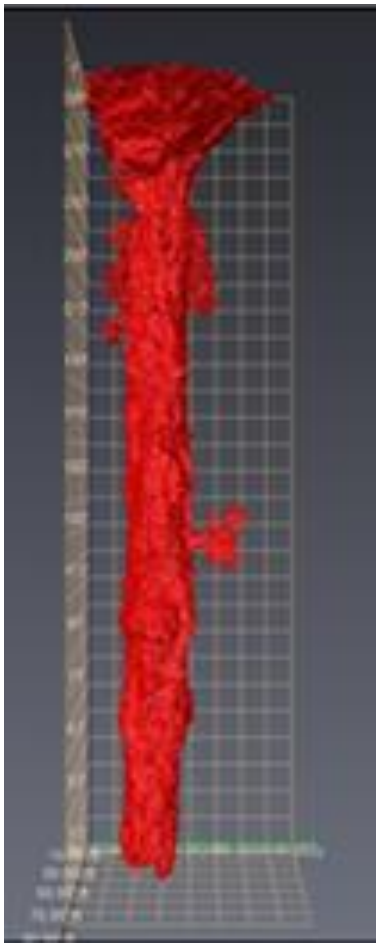

(c)

Figure S17. Test No. 18 (Series EW): view from the top (a), XCT image of the perforated concrete core (b), and 3D view of the perforation channel (c)

(a)

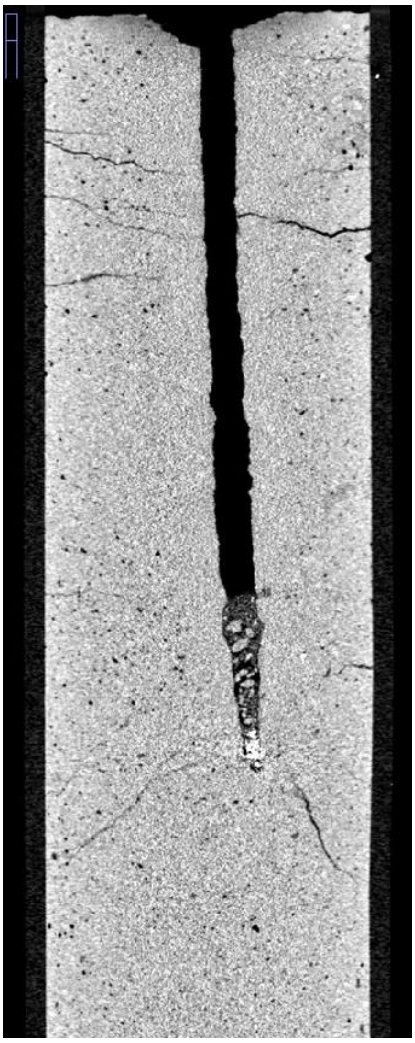

(b)

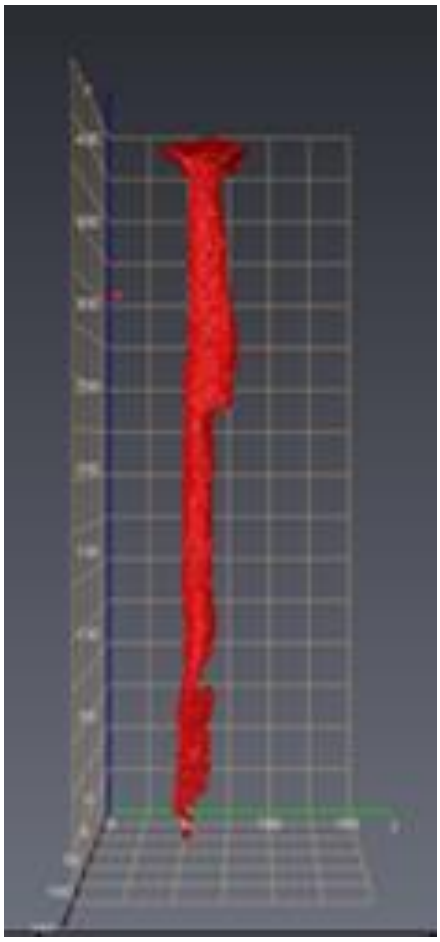

(c)

Figure S18. Test No. 19 (Series EW): view from the top (a), XCT image of the perforated concrete core (b), and 3D view of the perforation channel (c)

(a)

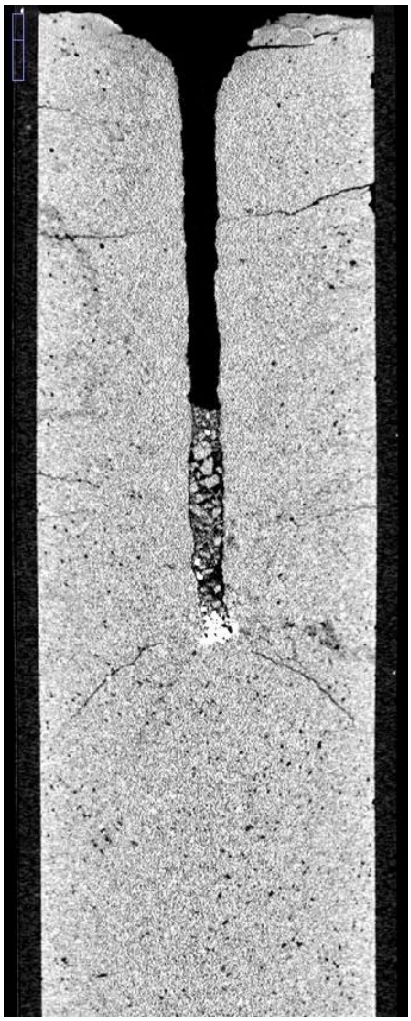

(b)

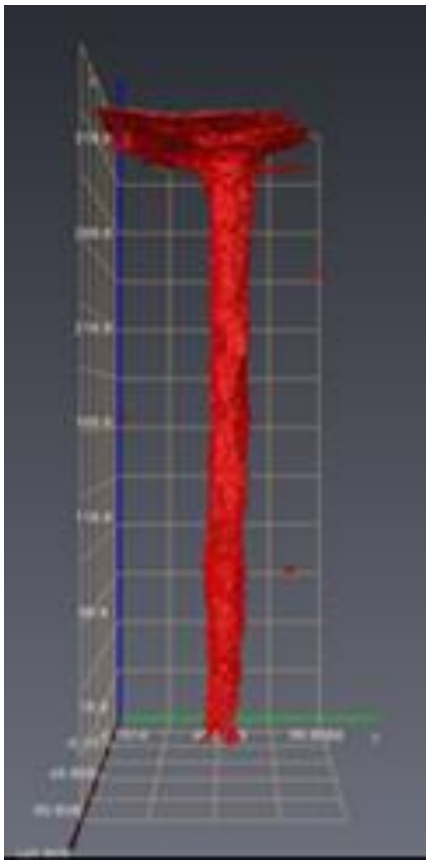

(c)

Figure S19. Test No. 20 (Series EW): view from the top (a), XCT image of the perforated concrete core (b), and 3D view of the perforation channel (c)

(a)

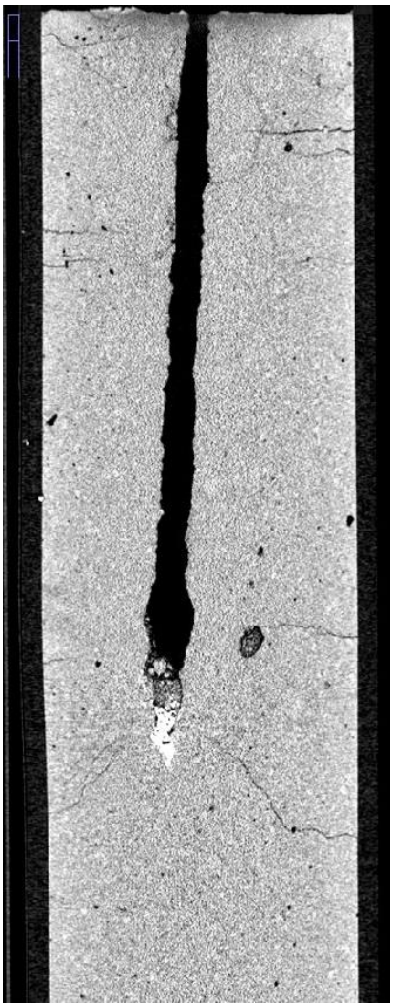

(b)

(c)

Figure S20. Test No. 21 (Series EW): view from the top (a), XCT image of the perforated concrete core (b), and 3D view of the perforation channel (c)

(a)

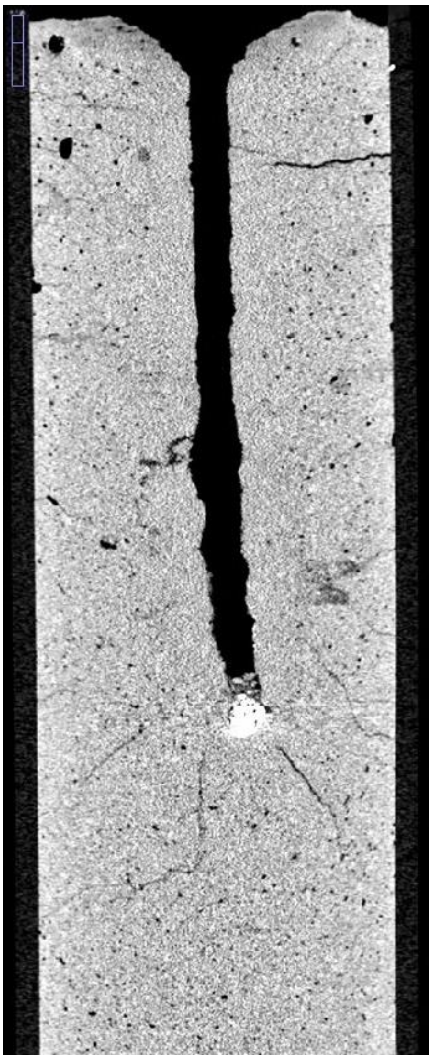

(b)

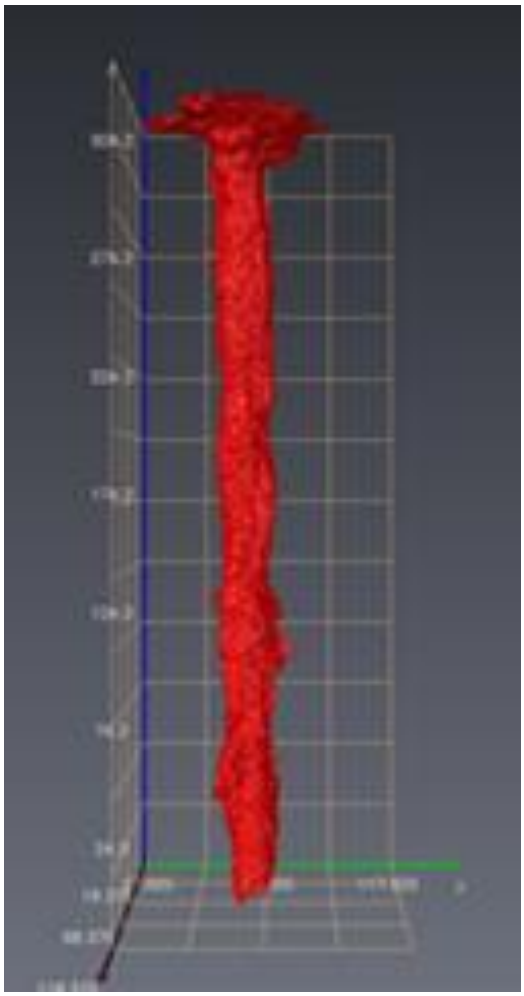

(c)

Figure S21. Test No. 22 (Series EW): view from the top (a), XCT image of the perforated concrete core (b), and 3D view of the perforation channel (c)

(a)

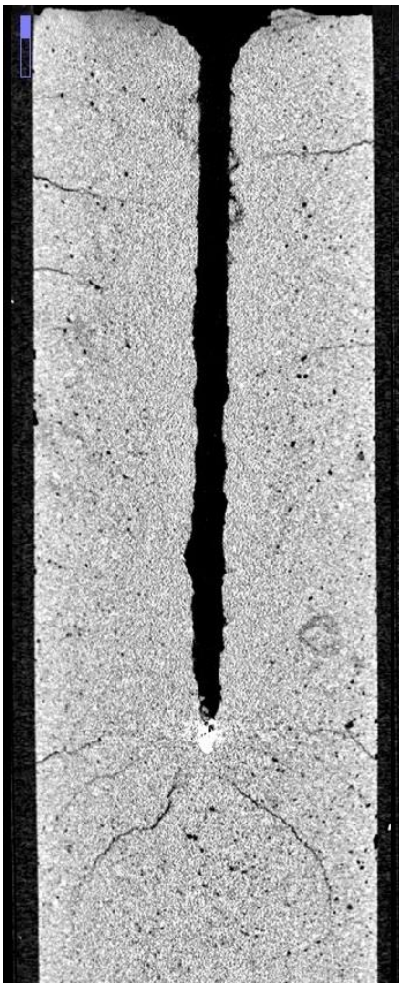

(b)

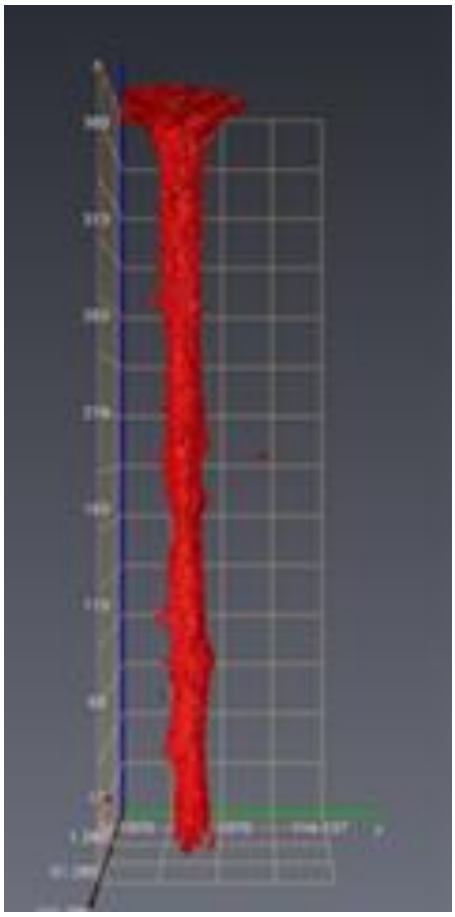

(c)

Figure S22. Test No. 23 (Series EW): view from the top (a), XCT image of the perforated concrete core (b), and 3D view of the perforation channel (c)

(a)

(b)

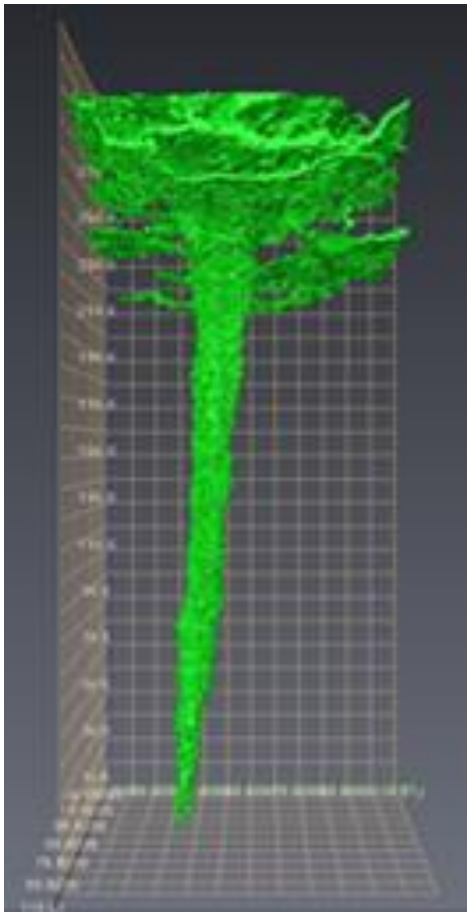

(c)

Figure S23. Test No. 24 (Series CP): view from the top (a), XCT image of the perforated concrete core (b), and 3D view of the perforation channel (c)

(a)

(b)

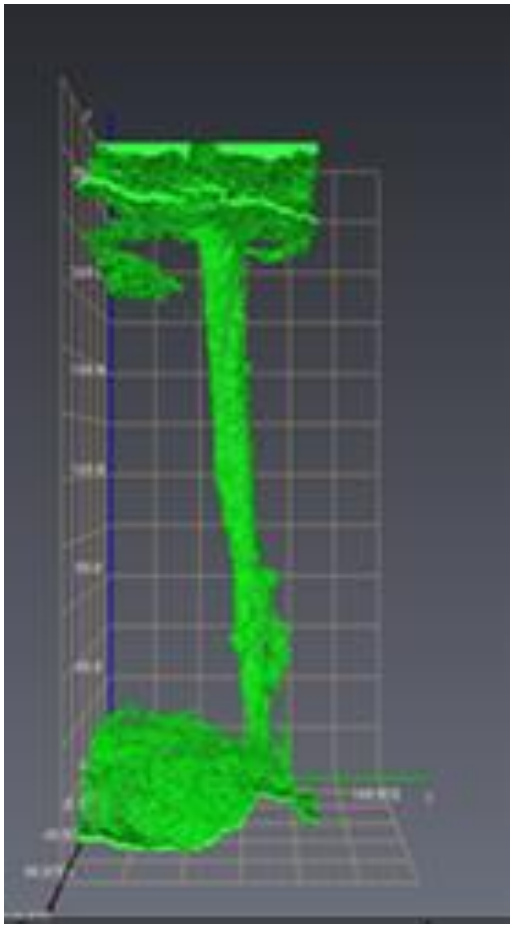

(c)

Figure S24. Test No. 25 (Series CP): view from the top (a), XCT image of the perforated concrete core (b), and 3D view of the perforation channel (c)

(a)

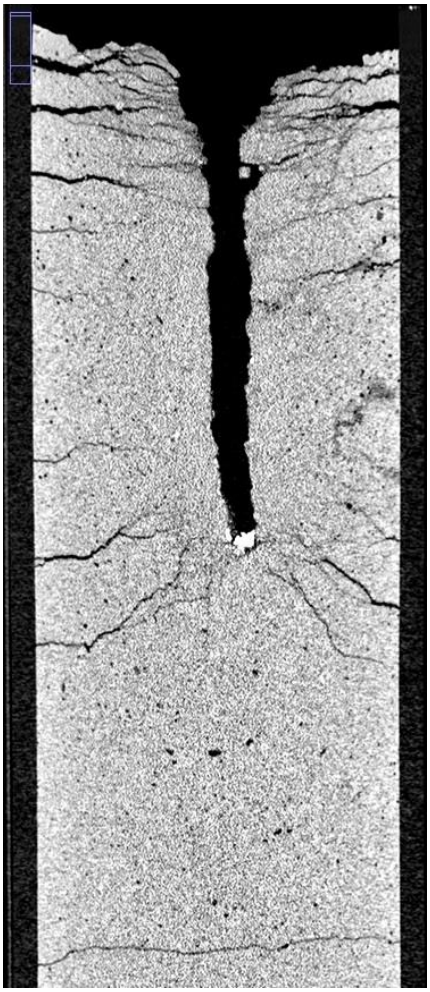

(b)

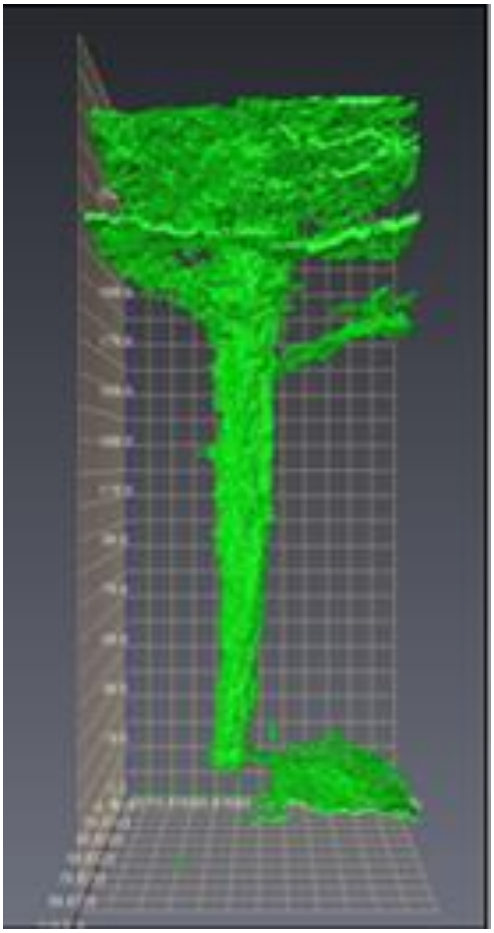

(c)

Figure S25. Test No. 26 (Series CP): view from the top (a), XCT image of the perforated concrete core (b), and 3D view of the perforation channel (c)

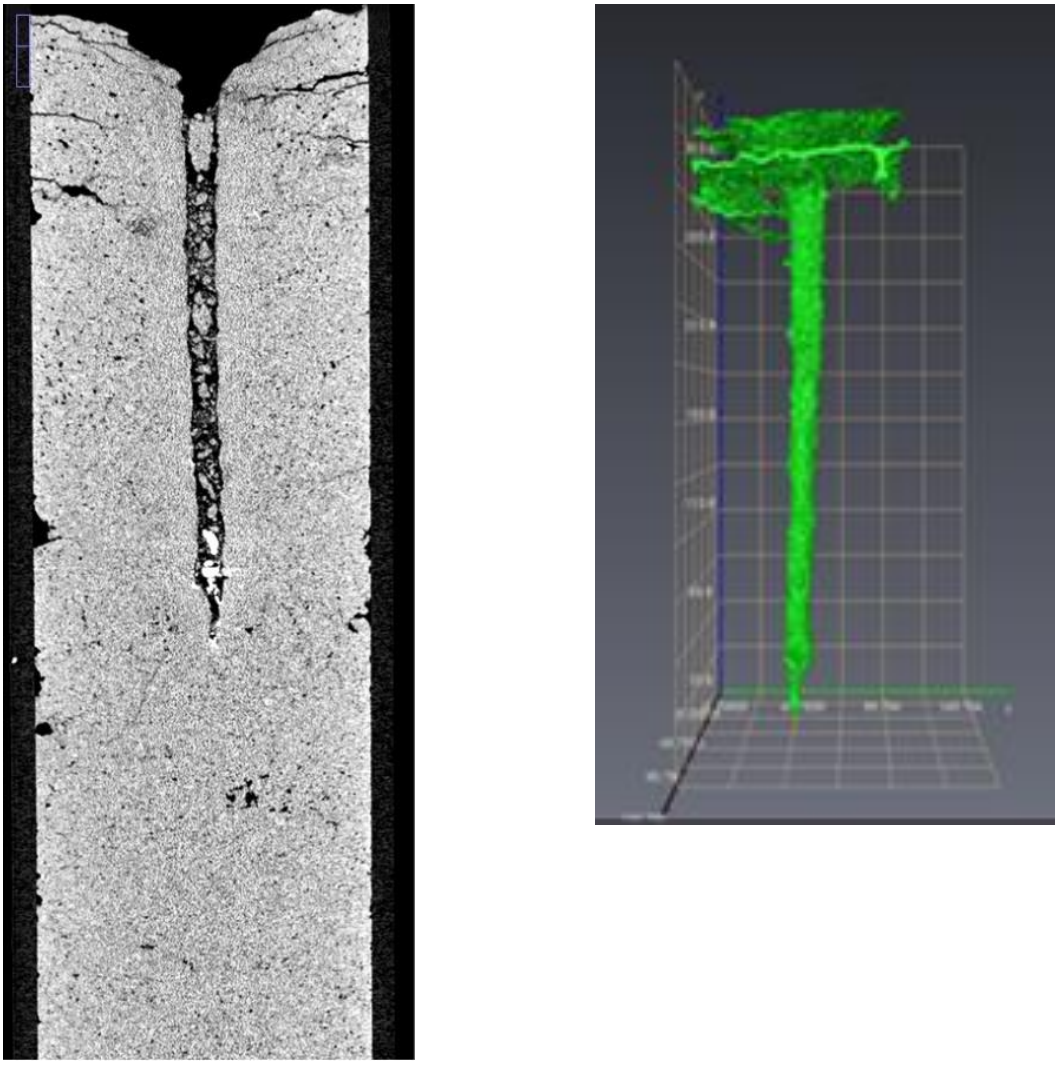

(a) (b)

Figure S26. Test No. 28 (Series CW): XCT image of the perforated concrete core (a), and 3D view of the perforation channel (b)

(a)

(b)

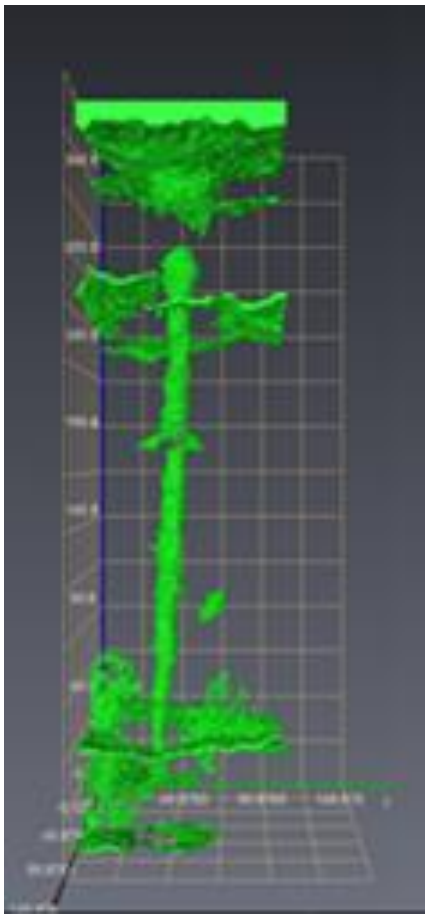

(c)

Figure S27. Test No. 29 (Series CW): view from the top (a), XCT image of the perforated concrete core (b), and 3D view of the perforation channel (c)

(a)

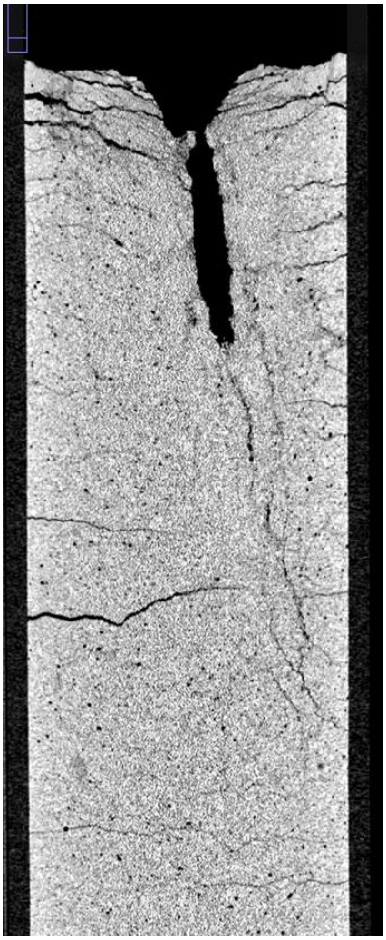

(b)

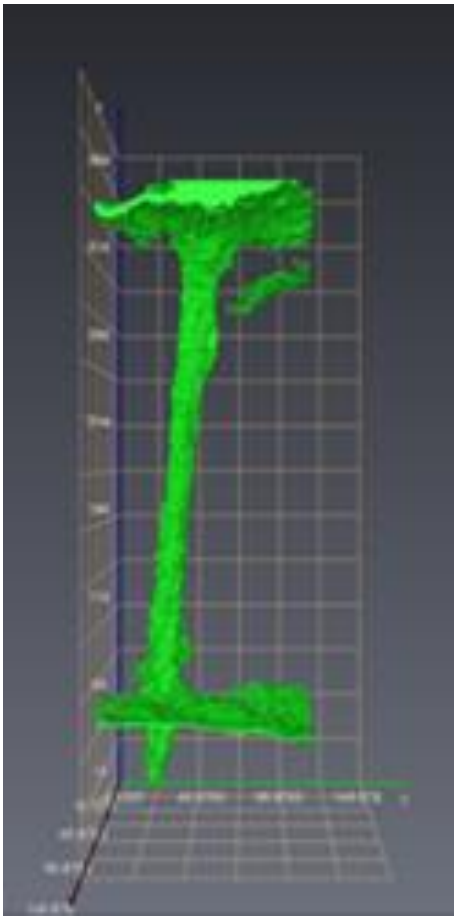

(c)

Figure S28. Test No. 30 (Series CW): view from the top (a), XCT image of the perforated concrete core (b), and 3D view of the perforation channel (c)

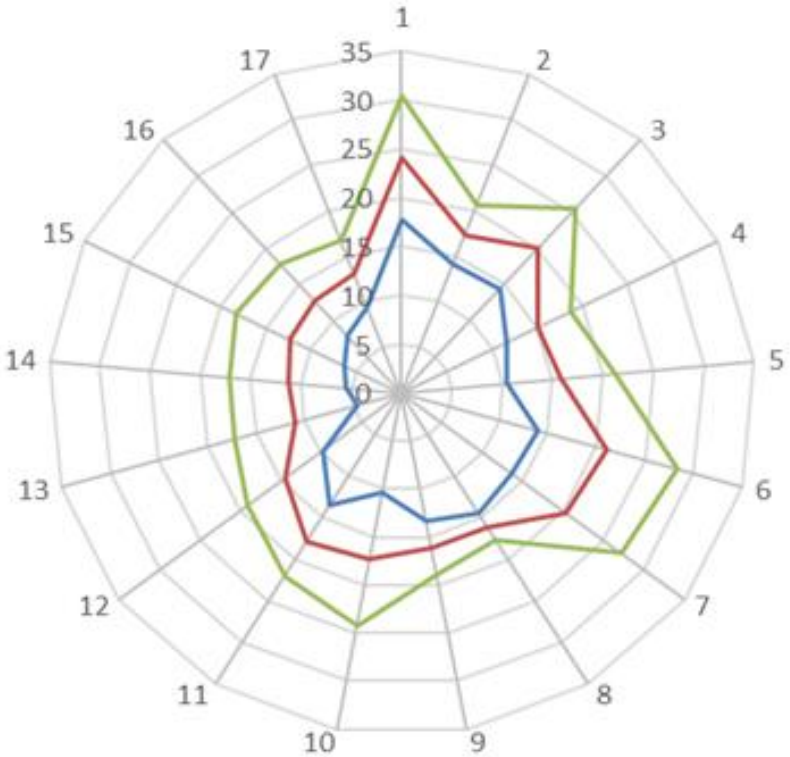

Figure S29. Irregularity of perforation channel for tests with use of a steel plate:

– minimum diameter of a given channel (blue, inner) [mm],

– maximum diameter of a given channel (green, outer) [mm],

–averaged value for the whole of the channel (red, in between) [mm]

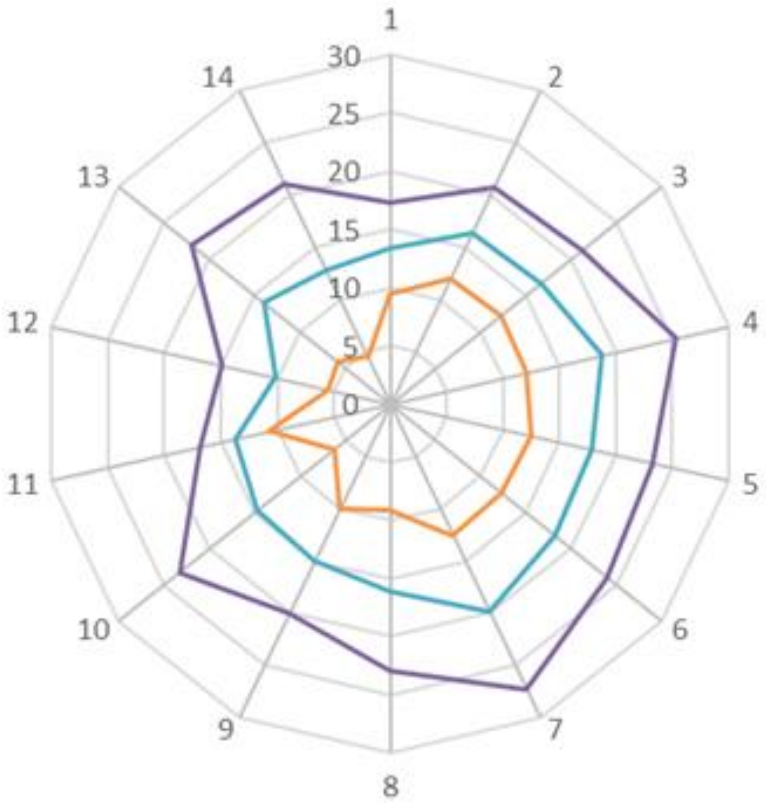

Figure S30. Change of perforation channels for tests without the use of a steel barrier:

– minimum diameter of a given channel (orange, inner) [mm],

– maximum diameter of a given channel (violet, outer) [mm],

– averaged value for the whole of the channel (blue, in between) [mm]

Central European Journal of Energetic Materials
ISSN 1733-7178; e-ISSN 2353-1843
Supplementary Information (SI) for *Cent. Eur. J. Energ. Mater.* **2020**, *17*(4): 584-599

(a) (b)

Figure S31. Views of the perforated steel control plates, used in the firing tests of (a) the tested, and (b) the commercial shaped charges

Received: January 28, 2020

First published online: December 31, 2020